

**Resonant formation of  $d\mu t$  molecules in deuterium:  
an atomic beam measurement of muon catalyzed  $dt$  fusion**

M. C. Fujiwara,<sup>1,2\*</sup> A. Adamczak,<sup>3</sup> J. M. Bailey,<sup>4</sup> G. A. Beer,<sup>5</sup> J. L. Beveridge,<sup>2</sup>  
M. P. Faifman,<sup>6</sup> T. M. Huber,<sup>7</sup> P. Kammel,<sup>8</sup> S. K. Kim,<sup>9</sup> P. E. Knowles,<sup>5†</sup>  
A. R. Kunselman,<sup>10</sup> M. Maier,<sup>5</sup> V. E. Markushin,<sup>11</sup> G. M. Marshall,<sup>2</sup> C. J. Martoff,<sup>12</sup>  
G. R. Mason,<sup>5</sup> F. Mulhauser,<sup>2†</sup> A. Olin,<sup>2,5</sup> C. Petitjean,<sup>11</sup> T. A. Porcelli,<sup>5‡</sup> J. Wozniak,<sup>13</sup>  
and J. Zmeskal<sup>14</sup>

(TRIUMF Muonic Hydrogen Collaboration)

<sup>1</sup>*Department of Physics and Astronomy, University of British Columbia, Vancouver, BC, Canada*

*V6T 2A6*

<sup>2</sup>*TRIUMF, Vancouver, Canada, V6T 2A3*

<sup>3</sup>*Institute of Nuclear Physics, 31-342 Krakow, Poland*

<sup>4</sup>*Chester Technology, Chester CH4 7QH, England, UK*

<sup>5</sup>*Department of Physics and Astronomy, University of Victoria, Victoria, BC, Canada V8W 2Y2*

<sup>6</sup>*Russian Research Center, Kurchatov Institute, Moscow 123182, Russia*

<sup>7</sup>*Department of Physics, Gustavus Adolphus College, St. Peter, MN 56082*

<sup>8</sup>*Department of Physics and Lawrence Berkeley National Laboratory, University of California,  
Berkeley, CA 94720*

<sup>9</sup>*Department of Physics, Jeonbuk National University, Jeonju City 560-756, S. Korea*

<sup>10</sup>*Department of Physics and Astronomy, University of Wyoming, Laramie, WY 82071-3905*

<sup>11</sup>*Paul Scherrer Institute, CH-5232 Villigen, Switzerland*

<sup>12</sup>*Department of Physics, Temple University, Philadelphia, PA 19122*

<sup>13</sup>*Faculty of Physics and Nuclear Techniques, University of Mining and Metallurgy, 30-059  
Krakow, Poland*

<sup>14</sup>*Institute for Medium Energy Physics, Austrian Academy of Sciences, A-1090 Vienna, Austria*

(October 31, 2018)

## Abstract

Resonant formation of  $d\mu t$  molecules in collisions of muonic tritium ( $\mu t$ ) on  $D_2$  was investigated using a beam of  $\mu t$  atoms, demonstrating a new direct approach in muon catalyzed fusion studies. Strong epithermal resonances in  $d\mu t$  formation were directly revealed for the first time. From the time-of-flight analysis of  $2036 \pm 116$   $dt$  fusion events, a formation rate consistent with  $0.73 \pm (0.16)_{meas} \pm (0.09)_{model}$  times the theoretical prediction was obtained. For the largest peak at a resonance energy of  $0.423 \pm 0.037$  eV, this corresponds to a rate of  $(7.1 \pm 1.8) \times 10^9$  s<sup>-1</sup>, more than an order of magnitude larger than those at low energies.

36.10.Dr, 21.45.+v, 25.60.Pj

Reactions of muonic hydrogen atoms and molecules present a sensitive testing ground for few-body theories involving strong, weak, and electromagnetic interactions. Among such reactions, muon catalyzed fusion ( $\mu\text{CF}$ ) in a deuterium–tritium mixture has attracted particular interest, where one muon can catalyze more than 100 nuclear fusions between deuteron and triton ( $d + t \rightarrow \alpha + n$ ) [1,2]. A key step in high-yield  $\mu\text{CF}$  is resonant formation [3] of the  $d\mu t$  molecule



where the collision energy, and the energy released upon formation of  $d\mu t$  in the loosely bound state ( $Jv = 11$ ), are absorbed in the ro-vibrational ( $K\nu$ ) excitation of the molecular complex  $[(d\mu t)dee]$ , a hydrogen-like molecule with  $(d\mu t)^+$  playing the role of one of the nuclei. Because of its limiting rate  $\lambda_{d\mu t}$ , the process has been considered one of the major bottlenecks in achieving high efficiency in  $\mu\text{CF}$ . However, theoretical calculations [4,5] predict strongly enhanced resonances for reaction (1) at  $\mu t$  kinetic energies of order 1 eV (epithermal resonances or ER), yet the experimental information is scarce thus far. It is the purpose of this letter to report a direct confirmation of the predicted ER and a determination of their energies, enabled for the first time with the atomic beam approach [6].

In conventional  $\mu\text{CF}$  experiments with homogeneous mixtures of hydrogen isotopes [1,2], the extraction of  $\lambda_{d\mu t}$  and its energy dependence relies on a kinetic model describing a complex chain of reactions, which includes processes that are not well understood, and assumptions that have been recently challenged (see Ref. [7]). The collision energy for reaction (1) in the equilibrium states is given by the target thermal energy, but difficulties in tritium handling have so far prevented realization of high temperature targets capable of thermally accessing ER. Although transient phenomena gave first evidence [8] and subsequent insight [9] into the epithermal effects in conventional targets, where a small fraction of  $d\mu t$  formation may occur before the thermalization, no quantitative measurement of  $\lambda_{d\mu t}$  for ER or its energy  $E_{res}$  has been obtained due primarily to unknown  $\mu t$  initial conditions.

The atomic beam method described here provides direct access to ER because of the

available  $\mu t$  beam energy (0.1–10 eV). A single  $d\mu t$  formation can be studied, on an event-by-event basis, isolated in time and space from other processes. With the  $\mu t$  time of flight (TOF) between the separated layers providing a measure of the collision energy,  $E_{res}$  can be determined in a direct manner. Furthermore, manipulation of heterogeneous multi-layers allows us to study and control, individually, important processes such as  $\mu$  transfer,  $\mu t$  emission, and moderation.

The experiment was performed at the M20B channel at TRIUMF. Details of the measurement and analysis may be found in Ref. [10]. The apparatus [11,12] is illustrated in Fig. 1. Target layers (Fig. 2(a)) were prepared by rapidly freezing a hydrogen isotope or mixture onto the gold foils, held at 3.5 K in an ultra-high vacuum of order  $10^{-9}$  torr or better. The layer thickness and uniformity were characterized off-line via energy loss of  $\alpha$  particles [12], and the effective thickness was then derived using a separate measurement [13] of the muon beam profile (about 30 mm diameter).

A beam of  $5 \times 10^3 \mu^- s^{-1}$  of momentum  $p=27$  MeV/ $c$  and momentum spread  $\Delta p/p=5.5\%$  (FWHM), defined by a 250  $\mu m$  scintillator of diameter 48 mm (T1), entered the target vacuum. It was degraded mainly by a 51  $\mu m$  gold foil upstream (US) from a TOF region. A fraction  $S_F$  of the  $\mu$  stopped in a tritium-doped hydrogen layer (an emission layer) of  $3.43 \pm 0.18$  mg·cm $^{-2}$  frozen to the US foil; most of these initially formed  $\mu p$ . The transfer  $\mu p \rightarrow \mu t$  took place in a time of typically 100 ns [14], creating  $\mu t$  with recoil energy of 45 eV due to the reduced mass difference. Because of the Ramsauer-Townsend effect in  $\mu t + p$  scattering,  $\mu t$  atoms are emitted with energies near 10 eV into an adjacent layer [13]. A D $_2$  moderation layer ( $96.0 \pm 5.0$   $\mu g \cdot cm^{-2}$ ) efficiently reduced the  $\mu t$  beam energy to  $\sim 1$  eV via elastic scattering in order to better match ER energies. The  $\mu t$ , after a flight time of a few  $\mu s$ , reached the D $_2$  reaction layer downstream (DS) from the TOF region ( $17.9 \pm 0.5$  mm from the US layers) and formed  $[(d\mu t)dee]$  from which fusion can occur to produce  $\alpha$  and  $n$ . The time between the  $\mu$  entrance signal and the detection of a fusion  $\alpha$  (which we call *fusion time*) is dominated by  $\mu t$  TOF and provides information on molecular formation energy, as long as the energy loss ( $\Delta E_{\mu t}$ ) of  $\mu t$ , due to elastic scattering before the formation in the DS

$D_2$ , is small. A thin DS layer of  $21.2 \pm 1.4 \mu\text{g}\cdot\text{cm}^{-2}$  was chosen to minimize  $\Delta E_{\mu t}$  so as not to obscure the time-energy correlation. The detailed theoretical description of our method is given in Ref. [15].

Two series of data, with emission layer tritium concentrations  $c_t = 0.1\%$  (Run 1) and  $c_t = 0.2\%$  (Run 2), were analyzed separately. Deuterium concentrations in  $H_2$  were typically less than 2 ppm. Run 1 had a  $1.77 \pm 0.12 \text{ mg}\cdot\text{cm}^{-2}$   $H_2$  substrate beneath the  $D_2$  DS reaction layer, while for Run 2 the  $D_2$  reaction layer was deposited directly on the DS gold foil. The data were normalized to the corrected number of incident muons,  $N_\mu$ , which takes into account the data acquisition dead time ( $\sim 20\%$ ) and pile-up of incident muons in the  $10 \mu\text{s}$  gate ( $\sim 5\%$ ). The signal and background in the Si detectors for Run 1 are shown in Fig. 2(b) with a delayed time cut selecting DS events, giving a S/B ratio of about 2:1. The background, mainly due to  $\mu$  decay and capture related processes (few fusion events from the US  $D_2$  moderator pass the delayed time cut because there is no TOF delay), can be accurately determined with the beam method from runs without the DS reaction layer, in which only DS fusion is turned off while other processes are not affected. Potential background from protons from  $\mu$ -induced  $dd$  fusion, arising for example from a recycled  $\mu$  following  $dt$  fusion, were estimated to give a  $2.4 \pm 0.9\%$  correction in DS fusion by looking at  $\alpha$ - $p$  correlations in the Si detectors, using the much larger data sample from fusion in the US moderation layer. A small contamination ( $\lesssim 5$  ppm) of nitrogen in the target layer was estimated to reduce the fusion yield by about 2%. Any further residual effects (*e.g.*, due to inaccuracy in the  $N_\mu$  scaler, or time zero shifts) were carefully investigated and were conservatively reflected in the final errors. With totals for  $N_\mu$  of  $6.02 \times 10^8$  and  $2.82 \times 10^8$  for the data and background runs, respectively, we have observed  $2036 \pm 116$  DS fusion events, for Runs 1 and 2 combined.

An absolute measurement of the fusion yield required determination of several factors including stopping fraction  $S_F$ , Si detector solid angle  $\Omega_{Si}$ , and energy and time cut acceptances,  $\epsilon_E$  and  $\epsilon_T$ . Our value of  $S_F = 0.299 \pm 0.015$  was based on fits of the decay electron time spectra recorded by electron and neutron counters (in the charged mode), where  $\mu$

stopped in H<sub>2</sub> exhibited a characteristic  $\sim 2 \mu\text{s}$  lifetime. The absolute efficiency of the counters was determined from the detection of delayed electrons following the observation of fusion [10].  $S_F$  then could be derived model-independently from the absolute amplitude at time zero of the  $2 \mu\text{s}$  decay electron component, normalized to  $N_\mu$ . An independent and consistent estimate of  $S_F$  was obtained from a GEANT [16] beam and decay simulation, which reproduced our measured range curve [17].

The energy cut efficiency and possible existence of tails in the  $\alpha$  energy distribution in the Si spectrum (Fig. 2(b)) were investigated by changing the cut width, as well as by simulating the energy loss of  $\alpha$  particles in the DS D<sub>2</sub> layer [18], giving  $\epsilon_E = 0.978 \pm 0.064$  for the applied cut of  $3.1 < E_\alpha < 3.7$  MeV.  $\Omega_{Si}$  was determined to be  $2 \times (2.46 \pm 0.10)\%$  from similar calculations, in which the spatial distribution of fusion events was constrained by electron imaging of muon decay. Effects of possible beam shifts [19] as well as small geometrical inaccuracies are reflected in the errors. After combining all the factors, including a small time cut correction, the absolute normalization was determined to the relative precisions of 9.5% and 7.7% for Runs 1 and 2, which together with statistical uncertainties gave the DS fusion yield per stopped  $\mu$  of  $(5.04 \pm 0.50) \times 10^{-4}/\mu$  and  $(4.27 \pm 0.54) \times 10^{-4}/\mu$  for Runs 1 and 2, respectively.

The results were used to test theoretical predictions as follows. The formation rate  $\lambda_{d\mu t}^{th}$  from Ref. [4], corrected for the Doppler broadening due to the target molecule motion at 3 K (without many-body effects), was used as a standard input, with low energy rates further modified to reflect possible sub-threshold effects [5]. The experimental TOF fusion distributions were fitted with a series of Monte Carlo (MC) simulated spectra for which the input  $\lambda_{d\mu t}$  and  $E_{res}$  were varied as  $\lambda_{d\mu t} = \mathcal{S}_\lambda \lambda_{d\mu t}^{th}$  and  $E_{res} = \mathcal{S}_E E_{res}^{th}$ . The measured absolute normalization and its estimated uncertainty were used to constrain the fit. The best values for  $\mathcal{S}_\lambda$  and  $\mathcal{S}_E$ , which were taken to be energy- and rate-independent, respectively, were extracted from the  $\chi^2$  distribution. The fusion probability  $W_f$  from Ref. [4] was kept fixed during the fit. A detailed simulation code was developed for the analysis [20]. Input cross sections for muonic processes were based on theoretical values in Refs. [21,22], but our multi-

layered target allowed independent tests of important reactions including  $\mu p \rightarrow \mu t$  transfer and  $p\mu p$  formation [14], and  $\mu t + p$  and  $\mu t + d$  collisions [10,13]. In addition, independent simulation codes [15,23] were used to check the consistency of some of the key processes. We stress the importance of explicitly treating the resonant scattering in the calculations; it can be shown [10] that the use of the renormalized effective rate  $\tilde{\lambda}_{d\mu t} \sim W_f \lambda_{d\mu t}$  as in Ref. [15] would result in the overestimate of the fusion yield by as much as a factor of two, a fact which resolves an earlier discrepancy reported in Ref. [6]. The effect of the energy distribution of resonantly scattered  $\mu t$  was investigated within the kinematically possible range. Solid state effects in thermalization and formation [24], which are important mostly at lowest energies, were not explicitly included in the simulations, but their influence at ER energies is expected to be small. The effects were estimated by appropriately modifying the cross sections. Table I summarizes our evaluation of systematic uncertainties in the MC modelling.

Figure 3 shows a comparison of the calculated MC spectrum with the data for Run 1. Also plotted are the simulated contributions from the time–energy correlated events (*i.e.* with small  $\Delta E_{\mu t}$ ), exhibiting more clearly the resonance structures due to different  $\nu$  states. From the fits, we obtained  $\mathcal{S}_\lambda = 0.88 \pm 0.11$  (Run 1) and  $0.55 \pm 0.12$  (Run 2) with  $\chi^2/\text{dof}$  ( $\text{dof} = 50$ ) of 0.96 and 1.27 respectively, and  $\mathcal{S}_E = 0.928 \pm 0.040$  (Run 1) and  $0.994 \pm 0.087$  (Run 2) with similar fit quality. The fit uncertainties reflect both statistical and normalization errors. An apparent deviation at the  $2\sigma$  level in  $\mathcal{S}_\lambda$  between Runs 1 and 2 may indicate some unaccounted-for systematic uncertainties (due possibly to slightly different experimental conditions as described above), hence the measurement error was increased accordingly so that two data set give  $\chi^2$  of 1 [25]. When the known MC modelling error (Table I) is included, the combined final result is  $\mathcal{S}_\lambda = 0.73 \pm (0.16)_{\text{meas}} \pm (0.09)_{\text{model}}$ . As for the resonance energy measurements, the weighted average of two runs gave  $\mathcal{S}_E = 0.940 \pm (0.036)_{\text{meas}} \pm (0.080)_{\text{model}}$ , where the modelling error is mainly due to uncertainties in the  $\mu t + d$  elastic scattering process and the  $\mu t$  TOF drift distance.

These scaling results correspond, in the theory [4], to a peak formation rate for the

main resonance ( $\nu=3$ ) of  $(7.1 \pm 1.8) \times 10^9 \text{ s}^{-1}$  at  $E_{res} = 0.423 \pm 0.037 \text{ eV}$  for  $\mu t^{F=1}$ , and  $(6.5 \pm 1.6) \times 10^9 \text{ s}^{-1}$  at  $0.508 \pm 0.047 \text{ eV}$  for  $\mu t^{F=0}$ , where  $F$  refers to the  $\mu t$  hyperfine state (the rates are normalized to liquid hydrogen density,  $4.25 \times 10^{22} \text{ cm}^{-3}$ ). The obtained rates are more than an order of magnitude larger than those at low energies [1], experimentally demonstrating the prospect for high cycling  $\mu\text{CF}$  in a high temperature target of several thousand degrees.

Our TOF sensitivity for the energy dependence allows us to clearly reject, for example, a constant  $\lambda_{d\mu t}$ , establishing the existence of resonant structure in epithermal  $d\mu t$  formation. If one assumes the energy level spectrum of the  $[(d\mu t)dee]$  molecule, our results for  $E_{res}$  imply sensitivity to the binding energy of the  $(d\mu t)_{11}$  state with an accuracy of the order of the vacuum polarization corrections.

We have recently collected data for resonant  $d\mu t$  formation in  $\mu t + \text{HD}$  collisions, for which the predicted resonances are even stronger [4,5]. The results of that measurement will be reported in a future publication [26].

We wish to thank C. Ballard, J. L. Douglas, K. W. Hoyle, R. Jacot-Guillarmod, and N. P. Kherani for their valuable help. The support of TRIUMF and its staff is gratefully acknowledged. M.C.F. would like to thank D. F. Measday for many helpful comments. This work was supported in part by NSERC (Canada), DOE and NSF (USA), and NATO Linkage Grant LG 930162.



## REFERENCES

- \* Present address: Department of Physics, Faculty of Science, University of Tokyo, Hongo, Tokyo 113-0033, Japan; e-mail: Makoto.Fujiwara@cern.ch.
- † Present address: Institute of Physics, University of Fribourg, CH-1700 Fribourg, Switzerland.
- ‡ Present address: Department of Physics, University of Northern British Columbia, Prince George, BC, Canada.
- [1] S. E. Jones *et al.*, Phys. Rev. Lett. **56**, 588 (1986); W. H. Breunlich *et al.*, *ibid.* **58**, 329 (1987); P. Ackerbauer *et al.*, Nucl. Phys. A **652**, 311 (1999).
- [2] For reviews see: W. H. Breunlich, P. Kammel, J. S. Cohen and M. Leon, Ann. Rev. Nucl. Part. Sci. **39**, 311 (1989); L. I. Ponomarev, Contemp. Phys. **31**, 219 (1990); P. Froelich, Adv. Phys. **41**, 405 (1992).
- [3] E. A. Vesman, JETP Lett. **5**, 91 (1967).
- [4] M. P. Faifman, L. I. Men'shikov and T. A. Strizh, Muon Catal. Fusion **4**, 1 (1989); M. P. Faifman and L. I. Ponomarev, Phys. Lett. **265B**, 201 (1991); M. P. Faifman *et al.*, Hyperfine Interact. **101/102**, 179 (1996).
- [5] Yu. V. Petrov, V. Yu. Petrov and H. H. Schmid, Phys. Lett. **331B**, 226 (1994); **378B**, 1 (1996).
- [6] G. M. Marshall *et al.*, TRIUMF Experiment 613; Z. Phys. C **56**, S44 (1992); Hyperfine Interact. **82**, 529 (1993); **101/102**, 47 (1996); **118**, 89 (1999).
- [7] B. Lauss *et al.*, Phys. Rev. Lett. **76**, 4693 (1996); P. Froelich and J. Wallenius, *ibid.* **75**, 2108 (1995); V. E. Markushin, Hyperfine Interact. **119**, 11 (1999).
- [8] J. S. Cohen and M. Leon, Phys. Rev. Lett. **55**, 52 (1985); P. Kammel, Nuovo Cimento Lett. **43**, 349 (1985).

- [9] V. E. Markushin *et al.*, *Hyperfine Interact.* **82**, 373 (1993); M. Jeitler *et al.*, *Phys. Rev. A* **51**, 2881 (1995).
- [10] M. C. Fujiwara, Ph.D. thesis, University of British Columbia (1999); M. C. Fujiwara *et al.*, to be published.
- [11] P. E. Knowles *et al.*, *Nucl. Instrum. Methods A* **368**, 604 (1996); *Hyperfine Interact.* **82**, 521 (1993).
- [12] M. C. Fujiwara *et al.*, *Nucl. Instrum. Methods A* **395**, 159 (1997); *Hyperfine Interact.* **101/102**, 641, (1996).
- [13] M. C. Fujiwara *et al.*, *Hyperfine Interact.* **118**, 151 (1999); **106**, 257 (1997).
- [14] F. Mulhauser *et al.*, *Phys. Rev. A* **53**, 3069 (1996).
- [15] V. E. Markushin, *Hyperfine Interact.* **101/102**, 155 (1996); PSI preprint PSI-PR-94-38 (1994).
- [16] GEANT 3.21, CERN Geneva (1993).
- [17] We note that the commonly used method of estimating  $S_F$  from relative amplitudes of a multi-lifetime fit ( $H_2$  versus Au) in the decay electron time spectrum gave an inconsistent result, which we attribute to a low energy background related to  $\mu$  capture on Au.
- [18] M. C. Fujiwara, APEC-97 and PEPPER (unpublished).
- [19] These cancel to first order for the  $x$  direction due to the symmetry of the two detectors.
- [20] T. M. Huber, SMC Monte Carlo code (unpublished); T. M. Huber *et al.*, *Hyperfine Interact.* **118**, 159 (1999).
- [21] L. Bracci *et al.*, *Muon Catal. Fusion* **4**, 247 (1989); C. Chiccoli *et al.*, *ibid.* **7**, 87 (1992).
- [22] M. P. Faifman, *Muon Catal. Fusion* **4**, 341 (1989).

- [23] J. Wozniak *et al.*, *Hyperfine Interact.*, **101/102**, 573 (1996).
- [24] P. E. Knowles *et al.*, *Phys. Rev. A* **56**, 1970 (1997) [Erratum: **57**, 3136 (1998)]; K. Fukushima, *ibid.* **48**, 4130 (1993); A. Adamczak, *Hyperfine Interact.* **119**, 23 (1999).
- [25] Particle Data Group, *Eur. Phys. J. C* **3**, 9 (1998).
- [26] T. A. Porcelli, Ph.D. thesis, University of Victoria (1999); T. A. Porcelli *et al.*, to be published.

## TABLES

TABLE I. Estimated effects on rate scaling parameter  $\mathcal{S}_\lambda$  by the systematic uncertainties in the MC modelling.

MC error source	$\Delta\mathcal{S}_\lambda/\mathcal{S}_\lambda$ %
$\mu$ beam size	1.2
Nonuniform $\mu$ stopping (GEANT)	1.8
$\mu t$ TOF drift distance	2.6
$\mu p \rightarrow \mu t$ transfer, $p\mu p$ formation	5.6
$\mu t + d$ , $\mu t + t$ scattering, layer thickness	5.7
$\mu t + p$ RT minimum energy	1.1
Resonance Doppler widths in solid	8.0
Solid state and low energy processes (subthreshold resonances, slow thermalization, $\mu t$ energy after resonant scattering)	5.0
Total (in quadrature)	12.9

FIGURES

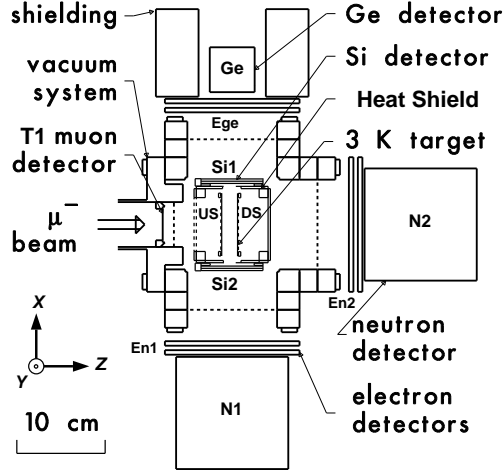


FIG. 1. Top view of the apparatus. Si detectors were placed in vacuum viewing target layers without a window, enabling the high resolution detection of fusion  $\alpha$  particles (Fig. 2(b)). The Ge detector monitored target impurities via muonic X-rays, while plastic scintillators (En1, En2, Ege) were used both to detect muon decay electrons and to veto charged particles for Ge and neutron (N1, N2) detectors.

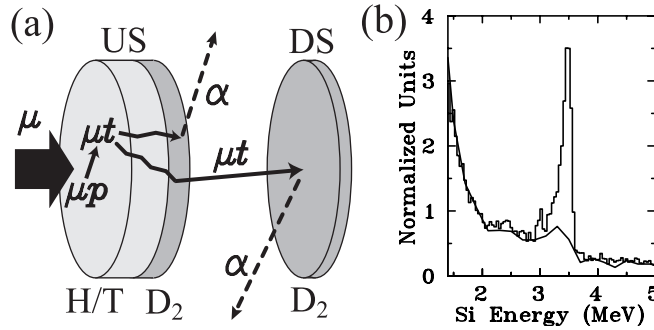


FIG. 2. (a) Schematic of the target consisting of emission, moderation, and reaction layers (not to scale). (b) Si energy spectra showing signal (histogram) and background (line) with a time cut of  $t > 1.5 \mu\text{s}$  selecting DS events delayed by  $\mu t$  TOF.

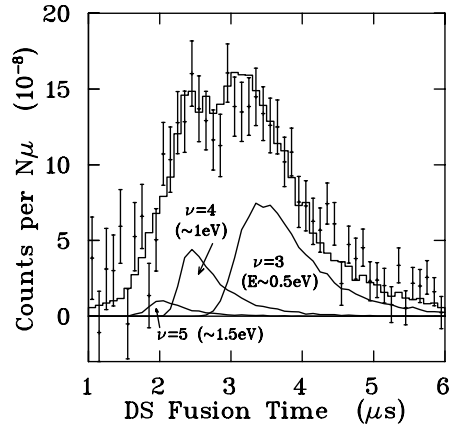


FIG. 3. Time-of-flight fusion spectrum (error bars) and simulation spectrum (histogram). Also plotted are simulated contributions from different resonance peaks given by time–energy correlated events with  $\Delta E_{\mu t} < 0.15$  eV. Note that angular dispersion of the  $\mu t$  beam also contributes to the peak widths.